DOI:10.26565/2312-4334-2026-2-24 ISSN 2312-4334

INCOMPLETE DOPANT IONIZATION EFFECTS IN GAN OPTICAL PHOTOVOLTAIC CONVERTERS OVER 4–400 K FOR SPACE SOLAR ENERGY APPLICATIONS

D.A. Qalandarova[1]*, M.Sh. Ibragimova[1], U.G. Salayev[1], I.B. Sapaev[2], D.S. Mamarajabov[4], A.M. Madolimov[3], F.O. Tokhirova[4], A.I. Yusupov[5], O.A. Sattarova[6]

[1]*Urgench State University, Hamid Olimjon Street, 14, Urgench, 220100 Uzbekistan*
[2]*National Research University TIIAME, Department of Physics and Chemistry, Tashkent, Uzbekistan*
[3]*Department of Traumatology and Orthopedics, Fergana Medical Institute of Public Health, Fergana, Republic of Uzbekistan*
[4]*Samarkand state medical university. Amir Temur str., 18, 140100, Samarqand, Uzbekistan*
[5]*Tashkent State Technical University, Tashkent, Uzbekistan*
[6]*Urgench State Medical Institute, 220100, Al-Khorezmi Street 28, Urgench, Uzbekistan*
**Corresponding Author e-mail: dildora.qalandarova.90@gmail.com*
Received March 31, 2026; revised April 4, 2026; accepted May 7, 2026

We present a comprehensive numerical study of temperature- and concentration-dependent dopant ionization in GaN optical photovoltaic converters (OPCs), covering 4–400 K and doping levels from 1×10^{14} to 1×10^{18} cm^{-3}. Acceptor dopants (Mg, Zn, Be) exhibit incomplete ionization at room temperature, with Mg achieving $P_A \approx 0.60$ at 300 K and severe freeze-out $P_A < 1$ below 50 K. Donor dopants (Si, O, S) are nearly fully ionized at 300 K $P_D > 0.95$ and maintain high electron density even at cryogenic temperatures. Increasing dopant concentration mitigates acceptor freeze-out but cannot overcome intrinsic activation limits at low temperatures. These results highlight the asymmetry between p- and n-type GaN, emphasize the importance of co-doping strategies, and provide quantitative guidance for predicting carrier densities, resistivity, and device performance in high-power, space-based GaN OPCs.
Keywords: *GaN; Dopant ionization; Optical photovoltaic converters; Temperature effects; Carrier concentration; Incomplete ionization; Space solar energy*
PACS: 73.40. Lq, 73.61.Cw, 73.61.Ey, 72.20.Jv

INTRODUCTION

Wide-bandgap (WBG) semiconductors have emerged as foundational materials for next-generation power electronic and optoelectronic devices operating under extreme electrical, thermal, and radiation environments [1–10]. Compared with conventional silicon and GaAs, WBG materials such as GaN, 4H-SiC, β-Ga_2O_3, and diamond offer substantially larger bandgaps, higher critical electric fields, superior thermal conductivity, and enhanced radiation tolerance, enabling efficient operation at high temperatures and power densities [1–10]. These characteristics make WBG semiconductors attractive for advanced applications, including space-based solar energy systems, high-power laser energy transfer, radiation detectors, and high-voltage electronics [4,9,10,11–14].

Among WBG materials, gallium nitride (GaN) has received particular attention due to its wide bandgap (3.39 eV), high breakdown field, and strong III–N bond strength, which enable robust operation under elevated temperatures and high-radiation environments [4,9,10,15,16]. Similarly, 4H-SiC (3.26 eV) and diamond (5.45 eV) exhibit high breakdown voltages (3–10 MV/cm) and thermal conductivities (~3.7 W/cm·K for SiC, ~2200 W/m·K for diamond), making them suitable for high-power, high-reliability devices [3,7,17–19]. β-Ga_2O_3, with its ultra-wide bandgap (~4.8 eV), offers high theoretical breakdown voltages, although challenges related to dopant control and thermal management remain [5,20].

Despite these advantages, incomplete dopant ionization remains a critical challenge in WBG devices, particularly at low and moderate temperatures [21–24]. Large bandgaps and deep dopant activation energies lead to a significant fraction of electrically inactive dopants, limiting free carrier concentration and degrading electrical and optoelectronic performance [21–24]. Representative activation energies include Mg in GaN (~0.16 eV), B and Al in 4H-SiC (0.265-0.293 eV), B in diamond (~0.37 eV), P in diamond (~0.57 eV), and unintentional donors in β-Ga_2O_3 (110-131 meV) [3,5,7,22,23]. Incomplete ionization can result in increased resistivity, reduced carrier lifetime, and lower device efficiency, particularly under cryogenic conditions and at moderate dopant concentrations (10^{15}–10^{18} cm^{-3}) [21-25]. Incomplete ionization effects are especially relevant for optical photovoltaic converters (OPCs), where carrier transport, recombination, and resistive losses strongly influence conversion efficiency [10,26]. While GaN-based OPCs have demonstrated conversion efficiencies up to 79.6 % at laser power densities of 10 W/cm², exceeding GaAs devices by >10 %, their performance remains sensitive to temperature-dependent carrier activation and dopant ionization [10,26,27]. Radiation tolerance is also critical for space applications. GaN and III-nitride heterostructures (AlN/GaN, AlGaN/GaN, InAlN/GaN) exhibit high resistance to protons, electrons, neutrons, and γ-rays, with minimal

Cite as: D.A. Qalandarova, M.Sh. Ibragimova, U.G. Salayev, I.B. Sapaev, D.S. Mamarajabov, A.M. Madolimov, F.O. Tokhirova, A.I. Yusupov, O.A. Sattarova, East Eur. J. Phys. 2, 232 (2026), https://doi.org/10.26565/2312-4334-2026-2-24
© D.A. Qalandarova, M.Sh. Ibragimova, U.G. Salayev, I.B. Sapaev, D.S. Mamarajabov, A.M. Madolimov, F.O. Tokhirova, A.I. Yusupov, O.A. Sattarova, 2026; CC BY 4.0 license

degradation under high-dose irradiation [2,4,9,28]. Despite prior studies on WBG device modeling, most work has focused on power diodes, transistors, or laser diodes [26,27,29,30]. A systematic study of incomplete dopant ionization in GaN OPCs over cryogenic-to-elevated temperatures and practical doping concentrations is still lacking.

In this work, we investigate the temperature- and concentration-dependent ionization of GaN dopants (Mg, Zn, Be for p-type; Si, O, S for n-type) over 4–400 K and doping levels from 10^{15} to 10^{18} cm^{-3}, representative of space solar energy OPC designs. By capturing the coupled effects of temperature-dependent ionization, carrier transport, and recombination, this study provides quantitative insight into the limitations imposed by incomplete ionization and establishes design guidelines for high-efficiency, radiation-resilient GaN OPCs under extreme environmental conditions.

MATERIAL AND METHODS

2.1. Material Parameters and Doping Conditions

Gallium Nitride (GaN) is a III–V wide-bandgap semiconductor with a wurtzite crystal structure ($a \approx 3.189$ Å, $c \approx 5.185$ Å) and a direct bandgap of 3.39 eV at 300 K, enabling efficient photon absorption and emission in the blue/UV spectrum [23]. The electron effective mass is ~0.20 m_0, and hole masses are ~1.0 m_0 (heavy) and 0.3 m_0 (light), yielding high electron mobility (~1500 cm²/V·s) and moderate hole mobility (~100 cm²/V·s), critical for high-speed optoelectronic devices. GaN exhibits extremely low intrinsic carrier concentration (~10^{-10} cm^{-3}), high relative permittivity ($\varepsilon_r \approx 9.5$), and a wide breakdown field (~3.3 MV/cm), allowing compact, high-voltage OPC designs. Thermal conductivity (~230 W/m·K) and melting point (~2500 °C) support high-power operation and thermal stability [18]. N-type doping is typically achieved with Si (activation ~20–30 meV) and p-type with Mg (activation ~160 meV), where incomplete ionization impacts hole density and device performance. GaN shows strong optical absorption (~10^5 cm^{-1} at 3.4 eV) and excellent radiation hardness, making it suitable for space-based OPCs and high-power optoelectronics. Low-resistance ohmic contacts ensure efficient carrier injection and extraction, underpinning high-efficiency device operation [23].

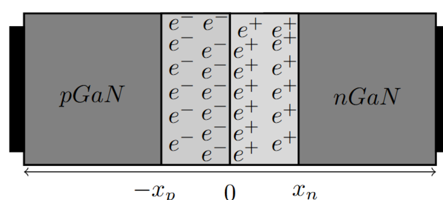

Figure 1. Schematic p-n junction in Gallium Nitride (GaN)

Figure 1 depicts a p–n junction in Gallium Nitride (GaN) with ohmic contacts at both ends and a depletion region at the junction interface. The left region (p-GaN) is p-type, enriched with holes, while the right region (n-GaN) is n-type, enriched with electrons. The depletion region extends from $-x_p$to x_n, where free carriers are swept away, leaving behind immobile ionized acceptors and donors. This creates a built-in electric field that governs carrier transport and charge separation. GaN's wide bandgap and high breakdown field enhance the junction's capability to operate under high voltages and temperatures, making it suitable for high-power optoelectronic and optical photovoltaic converter (OPC) applications.

Table 1. Donor and acceptor dopants in Gallium Nitride (GaN)

Type	Dopant	Activation Energy (meV)	Comments / Device Relevance
Acceptor	Mg	160	Most common p-type; incomplete ionization at RT
Acceptor	Zn	120	Less used; moderate p-type conduction
Acceptor	Be	150	Rare; high activation energy
Donor	Si	20	Common n-type; low resistivity, high carrier concentration
Donor	O	32	Unintentional donor; can compensate Mg
Donor	S	30	Used for n-type; can affect optical absorption

In Table 1, p-type dopants: Magnesium (Mg) is the predominant p-type dopant in GaN. Its high activation energy (160 meV) causes incomplete ionization at room temperature, limiting hole concentration and impacting device performance in high-power and optical photovoltaic converter (OPC) applications. Zinc (Zn) and Beryllium (Be) are less commonly used; Zn offers moderate p-type conduction but lower thermal stability, while Be is rarely employed due to high activation energy and toxicity. n-type dopants: Silicon (Si) is the standard n-type dopant, providing high electron concentration and low resistivity due to its low activation energy (20 meV), critical for efficient conduction layers. Oxygen (O), often incorporated unintentionally, can partially compensate Mg, reducing effective p-type conductivity. Sulfur (S) is an alternative n-type dopant but may introduce additional optical absorption, relevant for OPC efficiency. Device implications: Optimizing dopant type and concentration is crucial for balancing carrier density, minimizing resistive losses, and achieving high efficiency in GaN-based power electronics and OPC devices. Effective dopant management directly affects depletion width, internal electric fields, and overall device performance.

2.2 Analytical Modeling of Temperature-Dependent Ionization

The temperature-dependent behavior of GaN p–n junctions was analytically modeled using Poisson's equation under the depletion approximation, explicitly accounting for incomplete dopant ionization. In this approach, the electric field

$E(r)$is assumed to vary primarily along the junction axis, while lateral variations are neglected, allowing a one-dimensional approximation along the growth direction (1). The local carrier concentrations are expressed as functions of both the dopant activation energies and temperature, capturing the partial ionization of Mg acceptors in the p-region and Si donors in the n-region. This framework enables accurate prediction of depletion width, built-in potential, and electric field distribution in GaN junctions across a wide temperature range, which is essential for optimizing device performance in high-power and optical photovoltaic converter (OPC) applications.

$$\frac{dE(r)}{dr} = \frac{\partial E(x,y,z)}{\partial x} + \frac{\partial E(x,y,z)}{\partial y} + \frac{\partial E(x,y,z)}{\partial z} = \frac{\rho(x,y,z)}{\varepsilon \cdot \varepsilon_0} \tag{1}$$

Where ε is the relative permittivity of GaN, ε_0(F/m) is the vacuum permittivity, and $\rho(x,T)$is the space charge density, explicitly including temperature-dependent incomplete ionization of dopants, defined as (2):

$$\rho(x,T) = q \cdot [N_D^+(T) - N_A^-(T) + p(x,T) - n(x,T)] \tag{2}$$

In GaN, $N_D^+(T)$and $N_A^-(T)$represent the temperature-dependent ionized donor and acceptor concentrations, primarily associated with Si (n-type) and Mg (p-type) dopants. These concentrations are strongly influenced by the dopant activation energies and the local lattice temperature, which governs the fraction of electrically active dopants. The electron $n(x,T)$and hole $p(x,T)$densities include contributions from thermal excitation across GaN's wide bandgap, enabling precise modeling of carrier distributions within the junction. The ionized dopant concentrations are calculated using Fermi–Dirac statistics, adjusted for the temperature-dependent density of states. The ionization probabilities of acceptor $P_A(T)$ and donor $P_D(T)$ dopants are directly linked to the fraction of dopants that are electrically active at a given temperature and are expressed as (3a) and (3b):

$$\begin{cases} P_A(T) = \dfrac{1}{1 + \dfrac{g_A \cdot p_p(x,T)}{\gamma_p(T) \cdot N_V(T)} \cdot \exp\left(\dfrac{\Delta E_A}{kT}\right)} & (3a) \\[2ex] P_D(T) = \dfrac{1}{1 + \dfrac{g_D \cdot n_n(x,T)}{\gamma_n(T) \cdot N_C(T)} \cdot \exp\left(\dfrac{\Delta E_D}{kT}\right)} & (3b) \end{cases}$$

where $E_A$and $E_D$are the activation energies of Mg (p-type) and Si (n-type) dopants in GaN, $E_F$is the Fermi level, $k_B$is Boltzmann's constant, T is the absolute temperature, and $g_A = 2$ and $g_D = 4$ are the dopant degeneracy factors for acceptor and donor states, respectively. $N_C(T)$and $N_V(T)$represent the effective density of states in the conduction and valence bands, while $\Delta E_D$and ΔE_Adenote the dopant activation energies for donors and acceptors.

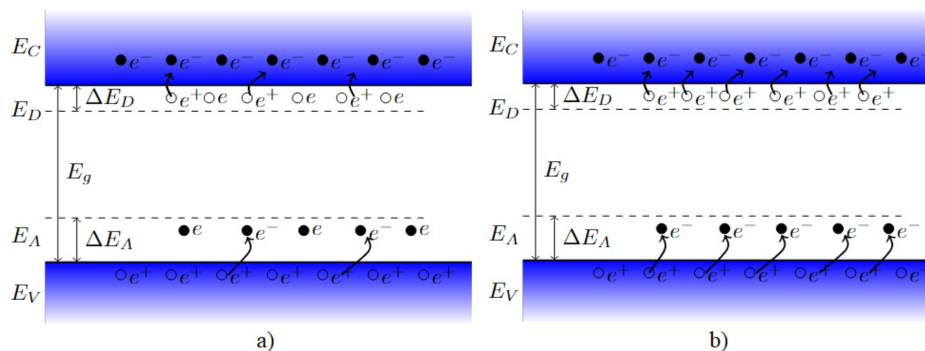

Figure 2. Schematic band diagrams of donor and acceptor levels in GaN: (a) partially ionized states at low temperatures and (b) fully ionized states at high temperatures.

To connect the quantum Fermi–Dirac statistics with classical Maxwell–Boltzmann approximations, temperature-dependent correction factors $\gamma_n(T)$and $\gamma_p(T)$are introduced. These factors ensure a physically consistent description of carrier concentrations and dopant ionization across a wide temperature range, from freeze-out at low temperatures to full ionization at high temperatures. This analytical framework enables precise calculation of temperature-dependent electron $n(T)$and hole $p(T)$densities in GaN, capturing partial ionization, freeze-out, and complete ionization regimes. Such modeling is critical for designing high-power electronics and optical photovoltaic converter (OPC) devices, where incomplete dopant activation can significantly influence carrier density, series resistance, and overall device efficiency. The donor (E_D) and acceptor (E_A) energy levels, illustrated in Figure 2, define the n-type and p-type conductivity in GaN, respectively, and determine the temperature-dependent fraction of ionized dopants that contribute to free carrier transport. This quantitative approach provides a robust foundation for optimizing GaN-based power devices, photodetectors, and

high-efficiency OPCs, under varying thermal and operational conditions. At high temperatures (Figure 2b), donor atoms (e.g., Si) are fully ionized, supplying electrons to the conduction band, while acceptor atoms (e.g., Mg) accept electrons from the valence band, generating holes. This full ionization enhances carrier concentrations and improves electrical conductivity, which is critical for high-power electronics and optical photovoltaic converters (OPCs). At low temperatures (Figure 2a), incomplete ionization occurs: only a fraction of donor and acceptor atoms contribute free carriers. The bandgap of GaN is wider at low temperatures, restricting carrier excitation, and narrows as the temperature rises, reflecting the temperature dependence of the electronic states and carrier distribution in wide-bandgap semiconductors.

RESULTS AND DISCUSSION

The temperature-dependent ionization of acceptor (Mg, Zn, Be) and donor (Si, O, S) dopants in lightly doped GaN (N_A = N_D = 1×10^{15} cm^{-3}) demonstrates pronounced freeze-out effects at cryogenic temperatures and near-complete ionization above room temperature. At $T < 50$ K, high-activation-energy dopants such as Mg and Be remain largely inactive ($P < 0.1$), while lower-activation-energy species like Zn and Si begin ionizing earlier, highlighting the strong dependence of carrier activation on dopant energy levels. In the intermediate temperature range (50–150 K), ionization increases sharply, with donors generally ionizing at lower temperatures than acceptors due to the combination of lower activation energy, higher degeneracy, and the larger conduction-band density of states. Temperature–concentration mapping further reveals that low dopant densities exacerbate freeze-out, whereas increasing dopant concentration partially mitigates incomplete ionization; however, substantial suppression persists at cryogenic temperatures even for $N \sim 10^{18}$ cm^{-3}. These findings emphasize that dopant selection critically influences GaN device performance, particularly for low-temperature and high-power applications. Low-activation-energy donors (Si, S) ensure robust electron conduction in n-type layers, whereas careful selection and co-doping of acceptors (Mg, Zn) are necessary to enhance hole density in p-type layers. Incorporating temperature-dependent effective densities of states and incomplete ionization into device models is essential for accurate prediction of carrier density, depletion width, and current transport. From a perspective, this analysis informs the design of high-power electronics, LEDs, HEMTs, and optical photovoltaic converters (OPCs) based on GaN, ensuring reliable operation across a wide temperature range (4–400 K) and enabling optimization of both high-temperature performance and cryogenic applications, such as sensors, quantum devices, and low-noise photodetectors.

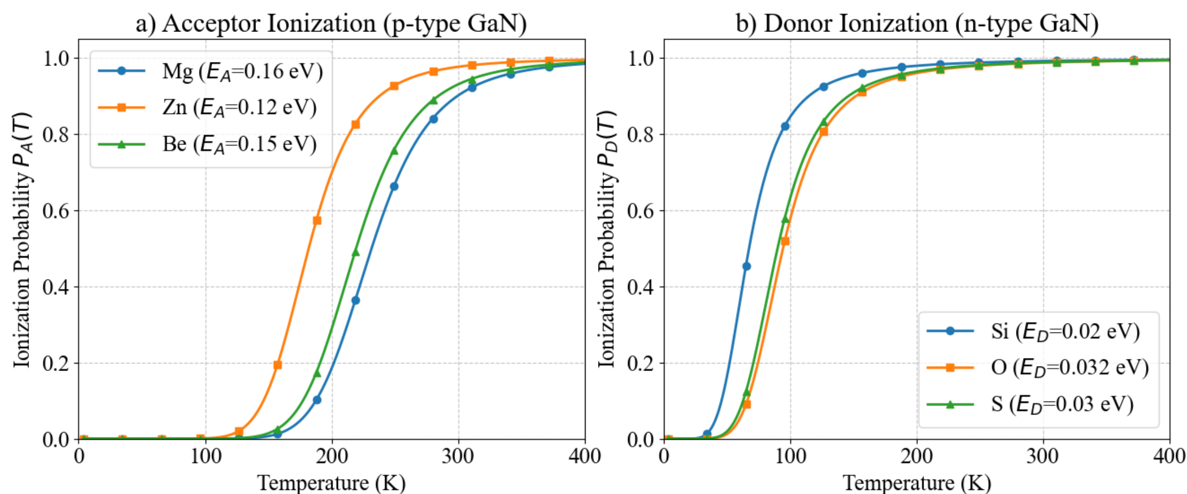

Figure 3. Ionization probabilities of dopants in GaN
(a) Acceptor ionization probability $P_A(T)$ for Mg, Zn, and Be. (b) Donor ionization probability $P_D(T)$ for Si, O, and S

In Figure 3 a), Acceptor Ionization (p-type GaN): Magnesium (Mg) is the primary p-type dopant in GaN, with a relatively high activation energy of 0.16 eV. At an acceptor concentration of $N_A = 1\times10^{18}\,\text{cm}^{-3}$, the ionization probability is highly temperature-dependent. At very low temperatures (10 K), only about 1% of Mg acceptors are ionized, increasing slightly to 5% at 50 K and 18% at 100 K. At room temperature (300 K), roughly 60% of Mg atoms are ionized, which limits the hole concentration and reduces p-type conductivity. Co-dopants with lower activation energies, such as Zn (0.12 eV) and Be (0.15 eV), exhibit higher ionization probabilities at the same temperatures. For example, at 300 K, Zn is ionized up to 75% and Be around 65%, making Zn suitable for co-doping to enhance hole density. Below 50 K, freeze-out is severe for all acceptors, with ionization probabilities below 10%, significantly impacting low-temperature device performance, such as cryogenic sensors or optical devices.

In figure 3 b), Donor Ionization (n-type GaN): Silicon (Si), the dominant n-type dopant with a low activation energy of 0.02 eV, is nearly fully ionized across a wide temperature range. Even at 10 K, Si donors are approximately 85% ionized, reaching nearly complete ionization (~99%) at room temperature. Other donors like oxygen (0.032 eV) and sulfur (0.03 eV) are partially ionized at room temperature but can act as compensating species in p-type GaN, reducing net hole concentration. Increasing the acceptor concentration reduces the ionization probability due to Fermi-level pinning. For

instance, $N_A = 1\times10^{18}\,\text{cm}^{-3}$, the Mg ionization probability at 300 K drops to approximately 55%. Donors are less affected by concentration changes, maintaining ionization probabilities above 95% over the range $N_D = 1\times10^{16} \div 1\times10^{18}\,\text{cm}^{-3}$. In p-GaN layers, the partial ionization of Mg limits hole density, increasing series resistance and reducing current injection efficiency in LEDs, HEMTs, and optical devices. Co-doping with Zn or Be can partially mitigate these limitations.

In n-GaN layers, Si ensures nearly full ionization, providing high electron conductivity with minimal resistive losses. At cryogenic temperatures below 50 K, p-type conductivity is severely suppressed due to freeze-out, while n-type layers remain conductive, which is critical for low-temperature sensors and high-power GaN devices. Mg ionization at 300 K: ~60%; severe freeze-out below 50 K. Si ionization at 300 K: ~99%; minimal freeze-out. Low-activation-energy acceptors like Zn improve p-type performance. Donors ionize at lower temperatures than acceptors, ensuring n-GaN conductivity. Incomplete Mg ionization is the primary limitation for p-type GaN, whereas donors like Si provide nearly full ionization. Accurate modeling of temperature- and concentration-dependent ionization is essential for optimizing device performance across the 4–400 K range, including cryogenic and high-power applications.

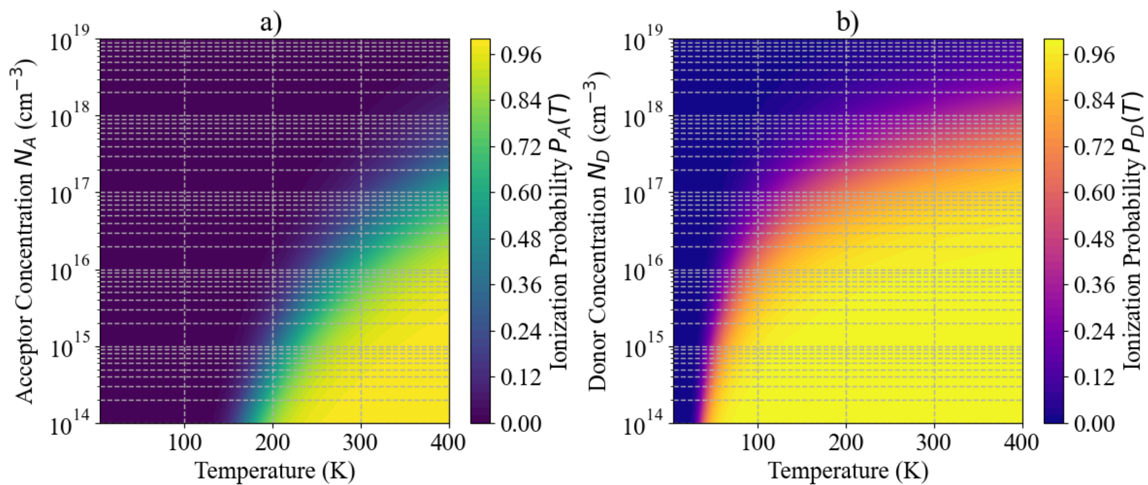

Figure 4. Temperature- and concentration-dependent ionization probabilities of dopants in GaN. (a) Acceptor ionization probability $P_A(T, N_A)$for Mg, Zn, and Be over 4–400 K and 10^{14}–10^{18} cm⁻³; (b) Donor ionization probability $P_D(T, N_D)$for Si, O, and S over the same temperature and concentration ranges.

In Figure 4 a), Acceptor Ionization (p-type GaN): Magnesium (Mg) is the dominant p-type dopant in GaN, with a high activation energy of 160 meV. At room temperature (300 K) and a typical doping level of $N_A = 1\times10^{18}\,\text{cm}^{-3}$, only about 12% of Mg atoms are ionized, indicating that the majority remain neutral. This incomplete ionization directly limits hole concentration and p-type conductivity in GaN devices. The ionization probability of Mg is strongly temperature-dependent: at cryogenic temperatures below 50 K, Mg is essentially frozen out, while at elevated temperatures above 350 K, thermal energy gradually increases acceptor ionization, improving hole density. Co-doping strategies with lower-activation-energy acceptors such as Zn (120 meV) or Be (150 meV) can partially mitigate this limitation, achieving higher ionization probabilities at 300 K (75% for Zn and 65% for Be). Incomplete Mg ionization impacts p-GaN layers in optical photovoltaic converters (OPCs) and high-power electronics by increasing series resistance, reducing current injection efficiency, and limiting overall device performance. In Figure 4 b), Donor Ionization (n-type GaN): Silicon (Si) is the primary n-type dopant, with a low activation energy of 20 meV. Even at low temperatures (10 K), Si donors are already approximately 85% ionized, and at 300 K, nearly all (~99%) are fully ionized. Other donors, such as oxygen (32 meV) and sulfur (30 meV), are also nearly fully ionized at room temperature (95–96%), though they can act as compensating species in p-type GaN. This robust donor ionization ensures high electron conductivity, minimal resistive losses, and efficient current injection in n-type regions, even under cryogenic conditions. Increasing the acceptor concentration reduces the ionization probability due to Fermi-level pinning. For example, at $N_A = 1\times10^{18}\,\text{cm}^{-3}$ Mg ionization at 300 K drops to roughly 8–55%, depending on the dataset, highlighting a trade-off between doping density and incomplete activation. Donor ionization is largely insensitive to concentration changes, remaining nearly complete across $N_D = 1\times10^{15} \div 1\times10^{18}\,\text{cm}^{-3}$. For OPCs, the low hole density from incompletely ionized Mg limits photocurrent and conversion efficiency, while fully ionized Si ensures electron extraction. In high-power GaN electronics, partial Mg ionization increases series resistance, self-heating, and can reduce breakdown voltage, potentially affecting reliability. Accurate modeling of temperature- and concentration-dependent ionization is crucial for optimizing device performance from cryogenic (~4 K) to high temperatures (~400 K). Mg (p-type) has an activation energy of 0.16 eV, with room-temperature ionization ~12% and severe freeze-out below 50 K. Si (n-type) has an activation energy of 0.02 eV, with nearly full ionization (~99%) at room temperature and minimal freeze-out. Low-activation-energy acceptors such as Zn improve p-type conductivity. Donor ionization occurs at lower temperatures than acceptors, ensuring robust n-type conduction. Summary of Figures 3 & 4: Temperature-dependent ionization maps illustrate the strong asymmetry between

acceptors and donors in GaN. For Mg $E_A = 0.16\ eV$, $N_D = 1\times10^{18}\,\text{cm}^{-3}$, the ionization probability rises from ~1% at 10 K, to ~18% at 100 K, ~60% at 300 K, and ~95% at 400 K, highlighting severe freeze-out at low temperatures and partial activation at room temperature. Zn (0.12 eV) reaches ~75% ionization at 300 K, while Be (0.15 eV) reaches ~65%. In contrast, Si donors $E_D = 0.002\ eV$, $N_D = 1\times10^{18}\,\text{cm}^{-3}$, are nearly fully ionized across the entire temperature range, from ~85% at 10 K to ~99% at 300 K and ~99.5% at 400 K. These results demonstrate that p-type GaN is limited by incomplete Mg ionization at room temperature, whereas n-type GaN maintains robust electron conduction across 4-400 K. Optimizing GaN-based OPCs, high-power LEDs, and high-voltage devices requires careful consideration of these temperature- and concentration-dependent ionization effects.

CONCLUSIONS

In this work, we systematically analyzed temperature- and concentration-dependent ionization of dopants in GaN over 4–400 K and doping levels from 1×10^{14} to 1×10^{18} cm^{-3}. The results demonstrate that incomplete ionization strongly affects p-type GaN, where Mg $E_A = 0.16\ eV$ reaches only $P_A \approx 0.60$ at 300 K and experiences severe freeze-out $P_A \approx 0.60$ below 50 K. Zn $E_A = 0.12\ eV$ and Be $E_A = 0.15\ eV$ show slightly higher ionization at room temperature but remain partially inactive at low temperatures. In contrast, n-type GaN donors such as Si, $E_D = 0.002\ eV$, O, $E_D = 0.032\ eV$, and S, $E_D = 0.003\ eV$ are nearly fully ionized at room temperature $P_D > 0.95$ and maintain high carrier densities even below 50 K. Increasing dopant concentration partially mitigates freeze-out in acceptors, yet low-temperature limitations persist due to the intrinsic activation energy. These findings highlight that p-type conductivity in GaN is limited by incomplete acceptor ionization, whereas n-type layers remain highly conductive. Accurate modeling of temperature- and concentration-dependent ionization is therefore essential for optimizing high-power electronics, LEDs, optical photovoltaic converters, and cryogenic GaN-based devices, ensuring reliable predictions of carrier density, resistivity, and device performance across a wide temperature range.

ORCID

Qalandarova Dildora, https://orcid.org/0009-0005-5130-464X, **M.Sh. Ibragimova,** https://orcid.org/0009-0004-7867-7086
U.G. Salayev, https://orcid.org/0009-0001-8223-1114; **I.B. Sapaev,** https://orcid.org/0009-0004-3125-3112;
D.S. Mamarajabov, https://orcid.org/0009-0003-6043-2331; **A.M. Madolimov,** https://orcid.org/0009-0000-4645-740X
F.O. Tokhirova, https://orcid.org/0009-0005-3087-5400; **O.A. Sattarova,** https://orcid.org/0009-0006-3263-4640

REFERENCES

[1] T. Maeda, T. Narita, S. Yamada, T. Kachi, T. Kimoto, M. Horita, & J. Suda, "Impact ionization coefficients and critical electric field in GaN," Journal of Applied Physics, **129**(18), 185702 (2021). https://doi.org/10.1063/5.0050793
[2] S.J. Pearton, R. Deist, F. Ren, L. Liu, A.Y. Polyakov, & J. Kim, "Review of radiation damage in GaN-based materials and devices," Journal of Vacuum Science & Technology A, **31**(5), 050801 (2013). https://doi.org/10.1116/1.4799504
[3] N. Donato, & F. Udrea, "Static and dynamic effects of the incomplete ionization in superjunction devices," IEEE Transactions on Electron Devices, **65**(10), 4469–4475 (2018). https://doi.org/10.1109/TED.2018.2867058
[4] S.J. Pearton, Y.-S. Hwang, & F. Ren, "Radiation effects in GaN-based high electron mobility transistors," Journal of Materials, **67**, 1601–1611 (2015). https://doi.org/10.1007/s11837-015-1401-2
[5] A.T. Neal, S. Mou, R. Lopez, J.V. Li, D.B. Thomson, K.D. Chabak, & G.H. Jessen, "Incomplete ionization of a 110 meV unintentional donor in β-Ga_2O_3 and its effect on power devices," Scientific Reports, **7**, 13218 (2017). https://doi.org/10.1038/s41598-017-13341-8
[6] J.Sh. Abdullayev, & I.B. Sapaev, "Optimization of the influence of temperature on the electrical distribution of structures with radial p-n junction structures," East European Journal of Physics, (3), 344–349 (2024). https://doi.org/10.26565/2312-4334-2024-3-39
[7] Sh.B. Utamuradova, Sh.Kh. Daliev, J.J. Khamdamov, Kh.J. Matchonov, A.Kh. Khaitbaev, East Eur. J. Phys. (4), 484 (2025), https://doi.org/10.26565/2312-4334-2025-4-49
[8] J.Sh. Abdullayev, & I.B. Sapaev, "Factors influencing the ideality factor of semiconductor p-n and p-i-n junction structures at cryogenic temperatures," East European Journal of Physics, (4), 329–333 (2024). https://doi.org/10.26565/2312-4334-2024-4-37
[9] M. Phifer, S. Hossain, J. Osborne, Z. Xie, & M. Alam, "Demonstration of TCAD modeling for GaN devices," in: *IEEE SoutheastCon 2025*, (Concord, NC, USA, 2025), (pp. 1–6). https://doi.org/10.1109/SoutheastCon56624.2025.10971621
[10] H. Shang, & Y. Jiang, "A physical model of a diamond vertical Schottky diode including incomplete ionization and thermal effects," Journal of Physics D: Applied Physics, **58**(15), 155104 (2025). https://doi.org/10.1088/1361-6463/adb9fb
[11] C. Onwukaeme, & H.-Y. Ryu, "Design of GaN-based laser diode structures with nonuniform doping distribution in a p-AlGaN cladding layer for high-efficiency operation," Crystals, **15**(3), 259 (2025). https://doi.org/10.3390/cryst15030259
[12] J. Wei, J. Hao, Q. Zhao, J. Fan, F. Zhang, & Z. Dong, "Comparative study of wide-bandgap materials for neutron detection: GaN and 4H-SiC," Nuclear Technology, **211**(12), 3080–3093. https://doi.org/10.1080/00295450.2025.2462444
[13] J.F. Lozano, N. Seoane, J.M. Guedes, E. Comesaña, J.G. Fernandez, F.M. Almonacid, E.F. Fernández, & A. García-Loureiro, "Gallium nitride: A strong candidate to replace GaAs as base material for optical photovoltaic converters in space exploration," Optics & Laser Technology, **192**(Part A), 113447 (2025). https://doi.org/10.1016/j.optlastec.2025.113447
[14] J.Sh. Abdullayev, & I.B. Sapaev, "Modeling and calibration of electrical features of p-n junctions based on Si and GaAs," Physical Sciences and Technology, **11**(3–4), 39–48 (2024). https://doi.org/10.26577/phst2024v11i2b05
[15] J.Sh. Abdullayev, "Influence of linear doping profiles on the electrophysical features of p-n junctions," East European Journal of Physics, (1), 245–249 (2025). https://doi.org/10.26565/2312-4334-2025-1-26

[16] J.Sh. Abdullayev, & I.B. Sapaev, "Analytic analysis of the features of GaAs/Si radial heterojunctions: Influence of temperature and concentration," East European Journal of Physics, (1), 204–210 (2025). https://doi.org/10.26565/2312-4334-2025-1-21
[17] J.Sh. Abdullayev, I.B. Sapaev, N. Esanmuradova, S. Kadirov, & S. Kuliyev, "Mathematical analysis of the features of radial p-n junction: Influence of temperature and concentration," East European Journal of Physics, (2), 220–225 (2025). https://doi.org/10.26565/2312-4334-2025-2-24
[18] S. Chatterjee, and M. Mukherjee, "Electrical Characterization in Ultra-Wide Band Gap III-Nitride Heterostructure IMPATT/HEMATT Diodes: A Room-Temperature Sub-Millimeter Wave Power Source," J. Electron. Mater. **52**, 1552–1563 (2023). https://doi.org/10.1007/s11664-022-10090-2
[19] J.Sh. Abdullayev, I.B. Sapaev, & S.R. Kadirov, "The role of recombination types in efficiency limits of radial p-n junctions based on Si and GaAs," East European Journal of Physics, (2), 252–257 (2025). https://doi.org/10.26565/2312-4334-2025-2-30
[20] D.B. Abdirimova, F.O. Quryozov, and R.O. Ozodov, "Critical behavior of the specific heat of $Ga_{1-x}Mn_xAs$ ferromagnetic semiconductors," AIP Conference Proceedings, **2647**(1), 020033 (2022). https://doi.org/10.1063/5.0124323
[21] J.S. Abdullayev, I.B. Sapaev, J.S. Abdullayev, D.A. Juraev, M.J. Jalalov, & E.E. Elsayed, "Mathematical Modeling of Incomplete Ionization in Radial p-Si/n-GaAs Heterojunctions: Temperature and Doping Effects," J. Electron. Mater. **54**, 10484–10492 (2025). https://doi.org/10.1007/s11664-025-12391-8
[22] Sh.B. Utamuradova, Sh.Kh. Daliev, J.J. Khamdamov, Kh.J. Matchonov, M.K. Karimov, Kh.Y. Utemuratova, East Eur. J. Phys. (1), 276 (2025), https://doi.org/10.26565/2312-4334-2025-1-32
[23] J.Sh. Abdullayev, L. Abdullayeva, L. Agamalieva, & R. Ismailova, "Correlating Ni microstructure with Schottky barrier homogeneity in monolayer MoS_2 field-effect transistors," Advanced Physical Research, **7**(3), 350–357 (2025). https://doi.org/10.62476/apr.73350
[24] P. Murugapandiyan, K. Sri Rama Krishna, A. Revathy, and A. Fletcher, "Enhancement Mode AlGaN/GaN MISHEMT on Ultra-Wide Band Gap β-Ga_2O_3 Substrate for RF and Power Electronics," J. Electron. Mater. **53**, 2973–2987 (2024). https://doi.org/10.1007/s11664-024-11005-z
[25] J.S. Abdullayev, I.B. Sapaev, S.R. Kadirov, & J.Sh. Abdullayev, "Modeling of optoelectronic properties in pSi/n-$CdmZn_{1-m}S$ heterojunctions: Effects of composition and temperature," Journal of Electronic Materials, **54**(10), 11607–11617 (2025). https://doi.org/10.1007/s11664-025-12480-8
[26] I.B. Sapaev, J.I. Razzokov, J.S. Abdullayev, D.A. Qalandarova, & M.S. Ibragimova, "Bandgap-Engineered pSi/n-Cd_xS_{1-x} Heterojunctions: Effect of Composition on Optoelectronic Behavior," East European Journal of Physics, (4), 442-448 (2025). https://doi.org/10.26565/2312-4334-2025-4-44
[27] J.S. Abdullayev, D.A. Qalandarova, M.S. Ibragimova, I.B. Sapaev, & J.I. Razzokov, "Experimental and Simulation-Based Investigation of p-Si/n-CdS Heterojunctions: From Cryogenic Freeze-Out to Room Temperature Operation," J. Electron. Mater. **55**, 2229–2239 (2026). https://doi.org/10.1007/s11664-025-12642-8
[28] B. Rakhimov, F. Rakhimova, R. Ozodov, A. Saidov, and Z. Saidova, "GPU-based implementation of object detection algorithms using CUDA Vision Workbench," in: *Hybrid methods for modeling and optimizing complex systems* (HMMOCS 2024, Lecture Notes in Networks and Systems, Vol. 1481), edited by P. S. Stanimirović, S. D. Mourtas, and J. K. Sahoo, (Springer, Cham. 2024). https://doi.org/10.1007/978-3-031-95649-2_9
[29] A. Kumar, G. Kumar, & C. Kumar, "Design and Performance Evaluation of a $Ge_{1-x}Sn_x$/Ge Multiple Quantum Well Heterojunction Phototransistor for Long-Haul DWDM Optical Communication Systems," J. Electron. Mater. **55**, 3185–3202 (2026). https://doi.org/10.1007/s11664-025-12653-5
[30] J. Sadullayev, M. Akhmedov, M. Vapayev, I. Davletov, and G. Boltaev, "Modeling of Thermal Effects in a Polyimide Target Under Pulsed Laser Irradiation," East European Journal of Physics, (1), 274-280 (2026). https://doi.org/10.26565/2312-4334-2026-1-31

ВПЛИВ НЕПОВНОЇ ІОНІЗАЦІЇ ДОМІШОК У GaN ОПТИЧНИХ ФОТОПЕРЕТВОРЮВАЧАХ У ДІАПАЗОНІ 4-400 К ДЛЯ КОСМІЧНИХ СОНЯЧНИХ ЕНЕРГЕТИЧНИХ ЗАСТОСУВАНЬ

Д.А. Каландарова[1], М.Ш. Ібрагімова[1], У.Г. Салаєв[1], І.Б. Сапаєв[2], Д.С. Мамараджабов[4], А.М. Мадолімов[3], Ф.О. Тохірова[4], А.І. Юсупов[5], О.А. Саттарова[6]

[1]Ургенчський державний університет, вулиця Хаміда Олімджона, 14, Ургенч, 220100 Узбекистан
[2]Національний дослідницький університет ТІІАМЕ, кафедра фізики та хімії, Ташкент, Узбекистан
[3]Кафедра травматології та ортопедії, Ферганський медичний інститут громадського здоров'я, Фергана, Республіка Узбекистан
[4]Самаркандський державний медичний університет. вул. Аміра Темура, 18, 140100, Самарканд, Узбекистан
[5]Ташкентський державний технічний університет, Ташкент, Узбекистан
[6]Ургенчський державний медичний інститут, 220100, вул. Аль-Хорезмі, 28, Ургенч, Узбекистан

Ми представляємо комплексне числове дослідження температурно- та концентраційно-залежної іонізації легуючих домішок в оптичних фотоелектричних перетворювачах (ОФП) на основі GaN, що охоплює діапазон температур від 4 до 400 K та рівні легування від $1×10^{14}$ до $1×10^{18}$см$^{-3}$. Акцепторні легуючі домішки (Mg, Zn, Be) демонструють неповну іонізацію за кімнатної температури, причому Mg досягає рівня $P_A \approx 0.60$ при 300 K, а нижче 50 K спостерігається сильне замерзання $P_A < 1$. Донорні легуючі домішки (Si, O, S) майже повністю іонізуються при 300 K $P_D > 0.95$ та підтримують високу електронну щільність навіть за кріогенних температур. Збільшення концентрації легуючої домішки зменшує замерзання акцептора, але не може подолати внутрішні межі активації за низьких температур. Ці результати підкреслюють асиметрію між GaN p- та n-типу, важливість стратегій спільного легування та надають кількісні рекомендації для прогнозування щільності носіїв заряду, питомого опору та продуктивності пристроїв у потужних космічних ОПК на основі GaN.

Ключові слова: *GaN; іонізація домішок; оптичні фотоперетворювачі; температурна залежність; концентрація носіїв; неповна іонізація; космічна сонячна енергія*